6ICEGE 6th International Conference on Earthquake Geotechnical Engineering
1-4 November 2015
Christchurch. New Zealand

Dissipated Energy in Undrained Cyclic Triaxial Tests

R.J.N. Azeiteiro [1], P.A.L.F. Coelho [2], D.M.G. Taborda [3], J.C. Grazina [4]

ABSTRACT

Energy-based methods are an emerging tool for the evaluation of liquefaction potential. These methods relate excess pore water pressure build-up to seismic energy dissipated per unit volume. Further development of these methods require their validation through laboratory testing. In this paper, a comprehensive study of energy dissipated during cyclic triaxial tests is undertaken. Results of undrained cyclic triaxial tests performed on air-pluviated samples of Hostun sand prepared with different initial densities and subjected to several confining pressures and loading amplitudes are presented. The energy dissipated per unit volume is estimated from the experimental results and correlated to the generated excess pore water pressure. The correlation between those quantities appear to be independent of the initial relative density of the sample, isotropic consolidation pressure and cyclic stress ratio used in the tests. Moreover, the relationship between observed double-amplitude axial strain and the energy dissipated per unit volume is examined. It is found that this relationship is greatly dependent on the relative density of the sample.

Introduction

Earthquake-induced soil liquefaction involves significant loss of the soil's strength and stiffness due to pore water pressure generation, which takes place concurrently with the dissipation of energy, mainly due to the rearrangement of soil's particles (Nemat-Nasser & Shokooh, 1979). The cumulative energy dissipated per unit volume of soil has been satisfactorily correlated to the pore water pressure build-up prior to the onset of liquefaction (e.g. Nemat-Nasser & Shokooh, 1979; Simcock *et al.*, 1983; Okada & Nemat-Nasser, 1994; Polito *et al.*, 2013) instigating the development of several energy-based approaches to evaluate site liquefaction potential (e.g. Davis & Berrill, 1982; Berrill & Davis, 1985; Figueroa *et al.*, 1994; Kokusho, 2013). According to Liang *et al.* (1995), when compared with stress-based or strain-based alternative procedures, approaches for the assessment of liquefaction potential based on energy offer some potential advantages, namely: (a) it is not necessary to decompose the erratic time-history of earthquake-induced stresses (or strains) to find an equivalent uniform loading; (b) the dissipated energy per unit volume depends on both stress and strain; (c) energy is a scalar quantity, which has the potential to simplify the liquefaction evaluation.

In this paper, a comprehensive study of energy dissipated during cyclic triaxial tests is undertaken. Results of undrained cyclic triaxial tests performed on air-pluviated samples of Hostun sand prepared with different initial densities and subjected to different confining pressures are presented. The energy dissipated per unit volume is determined from the

[1]PhD student, Dep. of Civil Engineering, University of Coimbra, Coimbra, Portugal, ricardoazeiteiro@uc.pt
[2]Assistant Professor, Dep. of Civil Engineering, University of Coimbra, Coimbra, Portugal, pac@dec.uc.pt
[3]Lecturer, Dep. of Civil and Environmental Engineering, Imperial College London, UK d.taborda@imperial.ac.uk
[4]Assistant Professor, Dep. of Civil Engineering, University of Coimbra, Coimbra, Portugal, graza@dec.uc.pt

experimental results and its correlation to excess pore water pressure generation and accumulated strain amplitude is thoroughly examined. Specifically, the effects of the confining pressure, void ratio and cyclic stress ratio (CSR) on those relationships are carefully investigated. The outcome of this experimental study intends to contribute to the further development of energy-based approaches for liquefaction assessement, in order to enhance its use in current practice.

Laboratory testing programme

Material and Equipment Used

All tests were performed on Hostun RF sand, which is a fine-grained, sub-angular to angular, silica sand (Flavigny *et al.*, 1990). In order to avoid segregation, the sand is uniformly graded between no. 20 (0.850 mm) and no. 200 (0.075 mm) sieves of ASTM series. The mean particle diameter, D_{50}, and the uniformity coefficient, C_u, are close to 0.33 mm and 1.4, respectively. The density of soil particles, G_s, is 2.64 and the minimum and maximum void ratios, e_{min} and e_{max}, are approximately 0.66 and 1.00, respectively (according to ASTM D4253-00 (2006) and ASTM D4254-00 (2006), respectively). Over the last decades, this sand has been used as a reference material for liquefaction studies (e.g. Konrad, 1993; Marques *et al.*, 2014).

A fully computer-controlled hydraulic triaxial apparatus of the Bishop & Wesley (1975) type, designed for 38 mm diameter specimens, was used to perform all tests. In order to apply extension loading, a flexible sleeve connecting a top cap to a reaction head was used. The instrumentation consisted of cell and pore water pressure transducers, a submersible load cell, an externally mounted LVDT and a volume gauge. The data provided by these instruments were continuously acquired by a data logger and transferred to a computer.

Experimental Procedures

Air-pluviation of dry sand was used to prepare all samples with a height/diameter ratio close to 2. Different relative densities were attained by varying the rate of pouring. For moderately loose samples, a miniature container was used, with the rate of pouring depending on the number and size of the openings. In the case of dense samples, the multiple sieving pluviation technique was used. Mass and volume measurements after preparation were performed to determine the density of the produced samples.

In order to minimise undesirable non-measured variations of the void ratio, a small suction of about 5 kPa was used to sustain the sample after dismounting the mould used during sand pluviation. Subsequently, during the saturation stage, the flow of de-aired water was induced by a small differential pressure (in general, lower than 5 kPa). A Skempton's B-value above 0.98 was measured in all tests before proceeding to the consolidation stage. All samples were isotropically consolidated to an effective pressure of 80 or 135 kPa (Table 1), before shearing.

Two different stages of undrained cyclic shearing were established by varying the axial stress only. In the first stage, the test was stress-controlled using a frequency of 1.5 cycles/h. As samples approached initial liquefaction and a hysteresis-type stress-strain behaviour became apparent, strain-controlled loading with reversal governed by a chosen deviatoric stress

amplitude was used, allowing a better control of the test. A constant axial strain rate of ±1 %/h was initially specified, being increased by two, four and eight times once the axial strain exceeded 0.5, 1 and 2 %, respectively. All samples were tested until large strains and excess pore water pressures were measured. Table 1 summarises the initial conditions of all conducted tests.

Table 1. Summary of the initial conditions of the cyclic triaxial tests performed

Test ID [§]	e_0 [‡]	σ'_0 (kPa) [‡]	Δq (kPa)	CSR = $\lvert\Delta q\rvert$ / (2 σ'_0)
ICUCT 0.803/80/0.225	0.803	80	± 36	0.225
ICUCT 0.832/80/0.250	0.832	80	± 40	0.250
ICUCT 0.804/80/0.300	0.804	80	± 48	0.300
ICUCT 0.793/135/0.250	0.793	135	± 67.5	0.250
ICUCT 0.579/80/0.250	0.579	80	± 40	0.250

[§] The designation identifies: 1) the type of consolidation – IC for isotropic consolidation; 2) the type of drainage –U for undrained test; 3) the type of loading –CT for cyclic triaxial loading; 4) the void ratio immediately after consolidation; 5) the isotropic consolidation stress; 6) the cyclic stress ratio (CSR).
[‡] Post-consolidation values.

Energy dissipated under undrained cyclic triaxial loading

The energy dissipated per unit volume of soil per loading cycle, W, can be determined using the area of the stress-strain hysteresis loop corresponding to that cycle, N. Although conceptually simple, difficulties can arise from the fact that the measured stress-strain loops are usually not closed (

Figure 1a). In order to overcome that problem, the following methodology was used in this study:

1) isolate each half-cycle stress-strain loop;
2) create a symmetric image of each half-cycle stress-strain loop about its centre;

centre the half stress-strain loop and its corresponding mirror image at the origin; an entire stress-strain loop is then defined by the original and the reflected half-loop (

3) Figure 1b);
4) estimate the area enclosed by each closed loop using a trapezoidal approximation (Equation (1)), which represents the energy dissipated per unit volume per loading cycle, W:

$$W = \int q\ \varepsilon_a \approx \sum_{i=1}^{k} \frac{1}{2}\left(q^{(i)} + q^{(i+1)}\right)\left({\varepsilon_a}^{(i+1)} - {\varepsilon_a}^{(i)}\right) \quad (1)$$

where q is the deviatoric stress, ε_a is the axial strain and k is the total number of points in which the stress-strain loop is discretised.

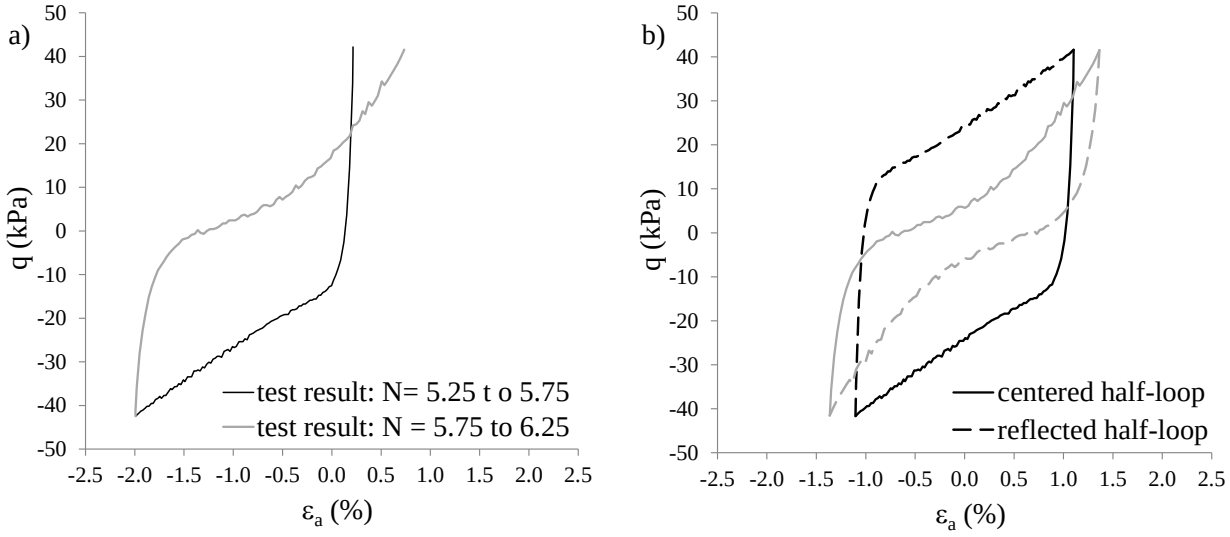

Figure 1. Methodology used for the estimation of the energy dissipated per unit of volume per loading cycle (ICUCT 0.832/80/0.250 test)

Experimental Results and Analysis

Residual Pore Water Pressure Build-up as a Function of Dissipated Energy

Figure 2a) presents the excess pore water pressure ratio generation, $r_u = \Delta u/\sigma'_0$, as a function of the number of loading cycles, N, for the ICUCT 0.832/80/0.250 test. As expected, r_u initially increases when subjected to compression loading, while decreasing under extension loading. Once the Phase Transformation line (Ishihara *et al.*, 1975) is crossed and the behaviour of sand changes from plastic contraction to plastic dilation and vice-versa, a double-frequency variation of r_u with N occurs (in the case of ICUCT 0.832/80/0.250 test, this can be observed from the 5th cycle of loading).

With the purpose of relating the excess pore water pressure generation to the dissipated energy, the values of r_u corresponding to a null deviatoric stress, i.e. the residual values, $(r_u)_{res}$, were computed (circle points shown in
Figure 2a). These values were then plotted against the accumulation of dissipated energy per unit volume, ΔW, normalised by the initial confining pressure, σ'_0, as presented in
Figure 2b). Due to the previously mentioned double-frequency variation of r_u with N, a significant fluctuation in the $(r_u)_{res} - \Delta W/\sigma'_0$ points can be observed for the last cycles of loading. This fluctuation leads to difficulties when comparing results of different tests. In order to overcome those difficulties, average values of $(r_u)_{res}$ were determined, with the obtained points being represented in
Figure 2b) as a function of $\Delta W/\sigma'_0$ accumulated after each cycle. By adopting this procedure, which is similar to that followed by Simcock *et al.* (1983), a smooth $(r_u)_{res} - \Delta W/\sigma'_0$ relationship is obtained.

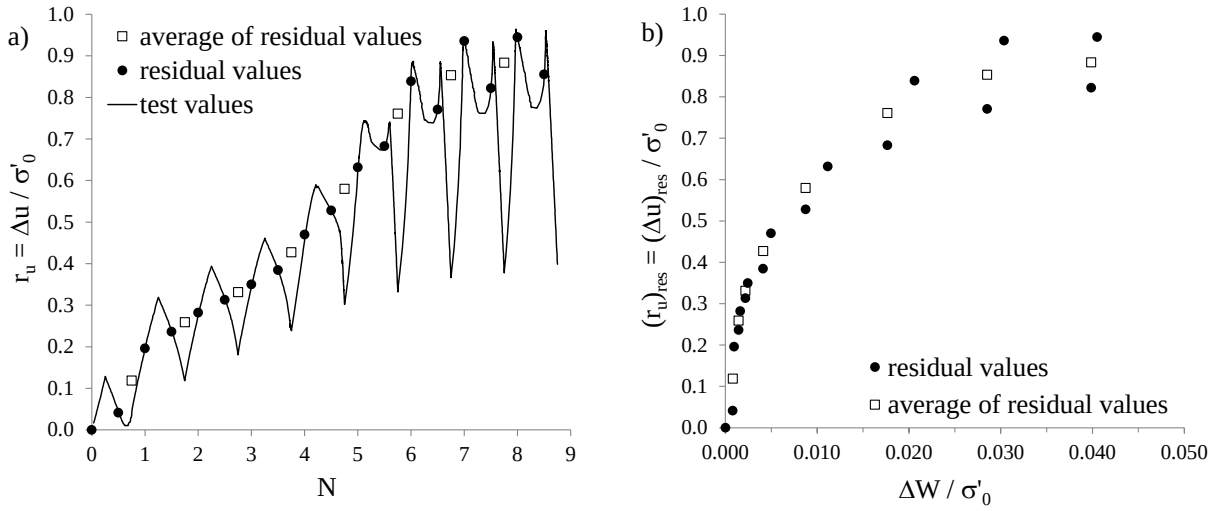

Figure 2. Excess pore water pressure ratio build-up as a function of a) the number of loading cycles and b) the normalised dissipated energy per unit volume in the ICUCT 0.832/80/0.250 test

Based on the aforementioned methodology, $(r_u)_{res} - \Delta W/\sigma'_0$ results obtained for the tests performed on samples with similar initial void ratio ($e_0 = 0.80 - 0.83$) and subjected to the same initial confining pressure ($\sigma'_0 = 80\ kPa$) were compared (Figure 3a). It can be observed that all samples show a similar excess pore water pressure generation, independent of the applied cyclic stress ratio (CSR), with minor differences being registered as double-frequency variation of r_u with N occurs. Similar findings were obtained by Polito *et al.* (2013) and Kokusho (2013) when analysing results of stress-controlled undrained cyclic triaxial tests on Ottawa 20/30 sand and Futtsu beach sand, respectively. Moreover, this conclusion seems to agree with that drawn by Figueroa *et al.* (1994) when examining strain-controlled torsional shear tests on Reid Bedford sand. These authors suggest that the influence of the shear strain amplitude on the amount of energy required to the onset of liquefaction can be neglected.

Figure 3b) compares the $(r_u)_{res} - \Delta W/\sigma'_0$ results obtained for a moderately loose (ICUCT 0.832/80/0.250) and a dense (ICUCT 0.579/80/0.250) samples, consolidated to the same isotropic stress state ($\sigma'_0 = 80\ kPa$) and subjected to the same oscillation of deviatoric stress ($\Delta q = \pm 40\ kPa$), and consequently, to the same $CSR = 0.250$. A similar generation of excess pore water pressure with accumulation of normalised dissipated energy can be observed, suggesting that the $(r_u)_{res} - \Delta W/\sigma'_0$ relationship is practically independent of the sample's density. This conclusion is also in good agreement with that reported by Kokusho (2013), when examining results of tests conducted on samples prepared with three different initial relative densities (30, 50 and 70%).

Finally, the $(r_u)_{res} - \Delta W/\sigma'_0$ results of two samples prepared to a similar initial void ratio ($e_0 = 0.79 - 0.83$) and subjected to the same cyclic stress ratio ($CSR = 0.250$), but submitted to a different isotropic consolidation pressure ($\sigma'_0 = 80$ and $135\ kPa$) are shown in Figure 3c). Minor differences seem to exist between the obtained results, suggesting that the

$(r_u)_{res} - \Delta W/\sigma'_0$ relationship is also independent of the consolidation stress level, at least when isotropic conditions are used, a behaviour which is similar to that observed by Kokusho (2013).

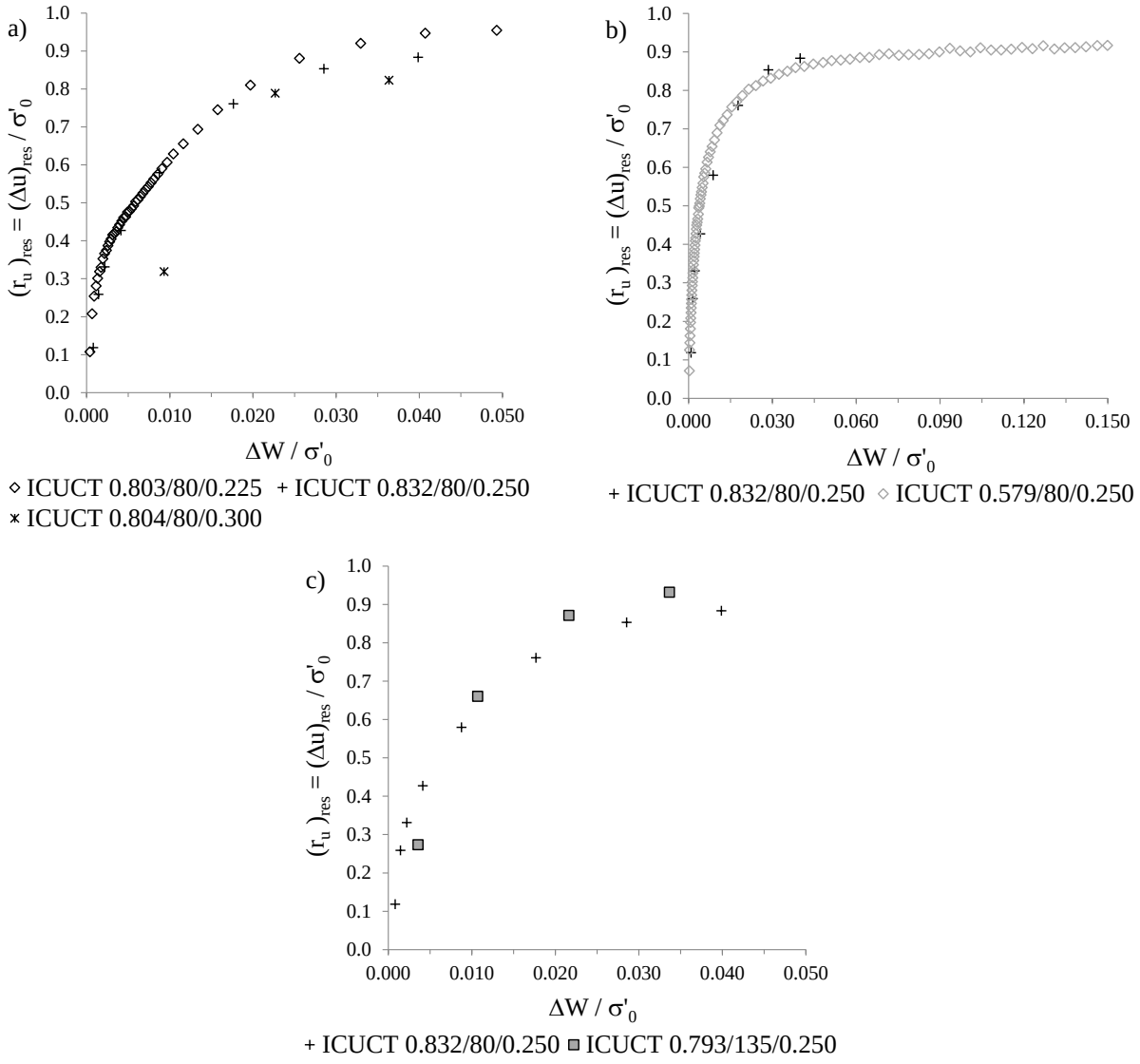

Figure 3. Influence of (a) CSR, (b) e_0 and (c) σ'_0 on the relationship between residual excess pore water pressure ratio build-up and normalised dissipated energy per unit volume

Double Amplitude Axial Strain as a Function of Dissipated Energy

Figure 4a), b) and c) show the influence of CSR, e_0 and σ'_0 on the relationship between the observed double-amplitude axial strain, ε_{DA}, and $\Delta W/\sigma'_0$, respectively. As suggested by Kokusho (2013), e_0 seems to have a major influence on the $\varepsilon_{DA} - \Delta W/\sigma'_0$ relationship. For a given value of $\Delta W/\sigma'_0$, the higher the value of e_0, the greater the observed ε_{DA} is (
Figure 4b). This suggests that initially looser samples require less energy (and, therefore, dissipate less energy) to achieve the same deformation of initially denser samples.

The $\varepsilon_{DA} - \Delta W/\sigma'_0$ relationship seems to be also affected by the CSR applied in the test (Figure 4a). Specifically, for the same $\Delta W/\sigma'_0$, the observed ε_{DA} seems to be larger for higher values of CSR. Conversely, the results presented in Figure 4c) suggests that the $\varepsilon_{DA} - \Delta W/\sigma'_0$ relationship is fairly independent of the isotropic consolidation pressure used.

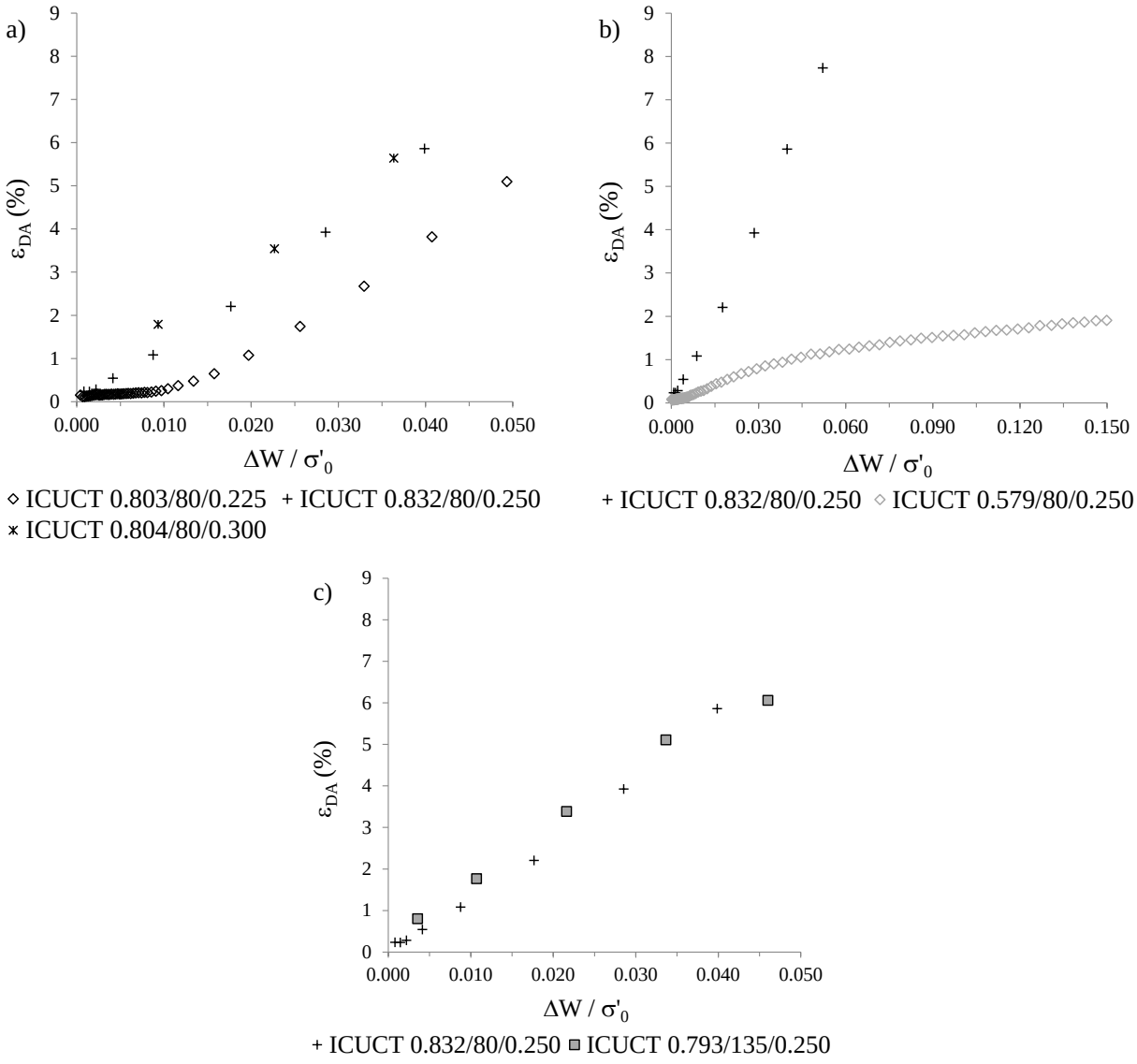

Figure 4. Influence of (a) CSR, (b) e_0 and (c) σ'_0 on the relationship between observed double-amplitude axial strain and normalised dissipated energy per unit volume

Conclusions

A series of undrained cyclic triaxial tests were performed on air-pluviated Hostun sand. Samples were prepared with different initial void ratio, isotropically consolidated to different confining

pressures and sheared under several cyclic stress amplitudes. The energy dissipated per unit volume was estimated from the experimental results and correlated to the average excess pore water pressure build-up and to the accumulation of double amplitude axial strain. The results suggest that the former relationship is practically independent of the initial void ratio, confining pressure and cyclic stress ratio (CSR).

The correlation between accumulation of double amplitude axial strain and energy dissipated per unit volume seems to be primarily affected by initial void ratio of the sample. For the same dissipated energy per unit volume, the observed double-amplitude axial strain is substantially higher when initially looser samples are tested. This relationship appears to be also affected by the CSR, while fairly independent of the isotropic consolidation pressure.

Acknowledgments

The authors would like to thank FCT – Fundação para a Ciência e a Tecnologia, Portugal, for sponsoring this research: Research Project PTDC/ECM/103220/2008 and grant no. SFRH/BD/84656/2012, supported by POPH – Programa Operacional Potencial Humano.

References

Berrill, J. B. & Davis, R. O. (1985). Energy dissipation and seismic liquefaction of sands: revised model. *Soils and Foundations*, **25**(2), 106–118.

Bishop, A. W. & Wesley, L. D. (1975). A hydraulic triaxial apparatus for controlled stress path testing. *Géotechnique*, **25**(4), 657–670.

Davis, R. O. & Berrill, J. B. (1982). Energy dissipation and seismic liquefaction in sands. Earthquake Engineering and Structural Dynamics, **10**, 59–68.

Figueroa, J. L., Saada, A. S., Liang, L. & Dahisaria, N. M. (1994). Evaluation of soil liquefaction by energy principles. *Journal of Geotechnical Engineering*, **120**(9), 1554–1569.

Flavigny, E., Desrues, J. & Palayer, B. (1990). Le sable d'Hostun «RF». *Revue Française de Géotechnique*, **53**, 67–69.

Ishihara, K., Tatsuoka, F. & Yasuda, S. (1975). Undrained deformation and liquefaction of sand under cyclic stresses. *Soils and Foundations*, **15**(1), 29–44.

Kokusho, T. (2013). Liquefaction potential evaluations: energy-based method versus stress-based method. Canadian Geotechnical Journal, **50**, 1088–1099.

Konrad, J.-M. (1993). Undrained response of loosely compacted and cyclic compression sands during monotonic tests. *Géotechnique*, **43**(1), 69–89.

Liang, L., Figueroa, J. L. & Saada, A. S. (1995). Liquefaction under random loading: unit energy approach. *Journal of Geotechnical Engineering*, **121**(11), 776–781.

Marques, A.S.P.S., Coelho, P.A.L.F., Haigh, S. & Madabhushi, G. (2014). Centrifuge modeling of liquefaction effects on shallow foundations. In Seismic Evaluation and Rehabilitation of Structures. *Geotechnical, Geological and Earthquake Engineering*, **26**, 425–440.

Nemat-Nasser, S. & Shokooh, A. (1979). A unified approach to densification and liquefaction of cohesionless sand in cyclic shearing. *Canadian Geotechnical Journal*, **16**, 659–678.

Okada, N., & Nemat-Nasser, S. (1994). Energy dissipation in inelastic flow of saturated cohesionless granular media. *Géotechnique*, **44**(1), 1–19.

Polito, C., Green, R. A., Dillon, E., & Sohn, C. (2013). Effect of load shape on relationship between dissipated

energy and residual excess pore pressure generation in cyclic triaxial tests. *Canadian Geotechnical Journal*, **50**, 1118–1128.

Simcock, K. J., Davis, R. O., Berrill, J. B. & Mullenger, G. (1983). Cyclic triaxial tests with continuous measurement of dissipated energy. *Geotechnical Testing Journal*, GTJODJ, **6**(1), 35–39.